Atmospheric Oxidation of Piperazine Initiated by OH: A Theoretical Kinetics Investigation

Zhonghua Ren, Gabriel da Silva*

Department of Chemical Engineering, The University of Melbourne, Parkville 3010, Australia.

*gdasilva@unimelb.edu.au

ABSTRACT

Piperazine (Pz) mixed with other amines is a proposed carbon capture solvent, but there is concern about the impact of Pz on air quality, including the potential to produce toxic products. Here, the •OH initiated oxidation of Pz has been studied by *ab initio* modelling and RRKM / master equation kinetic simulations. The Pz + •OH reaction is found to proceed at around the capture rate, consistent with experiment, with abstraction predominantly from C—H sites. The subsequent reaction kinetics of carbon centred Pz radicals with O_2 are also studied, so as to determine the first-generation oxidation products. We find that the Pz radical predominantly reacts with O_2 to produce a cyclic imine product + HO_2• under tropospheric conditions, with the stabilized peroxyl radical formed as a minor product. Subsequent reaction of the peroxyl radical with NO produces an alkoxyl radical that can react with O_2 to yield a cyclic amide or undergo unimolecular ring opening followed by a second O_2 addition / HO_2• elimination step to produce CH_2=NCH_2CH_2NHCHO.

KEYWORDS

Atmospheric chemistry, kinetics, piperazine, transition state theory, computational chemistry

TOC Graphic

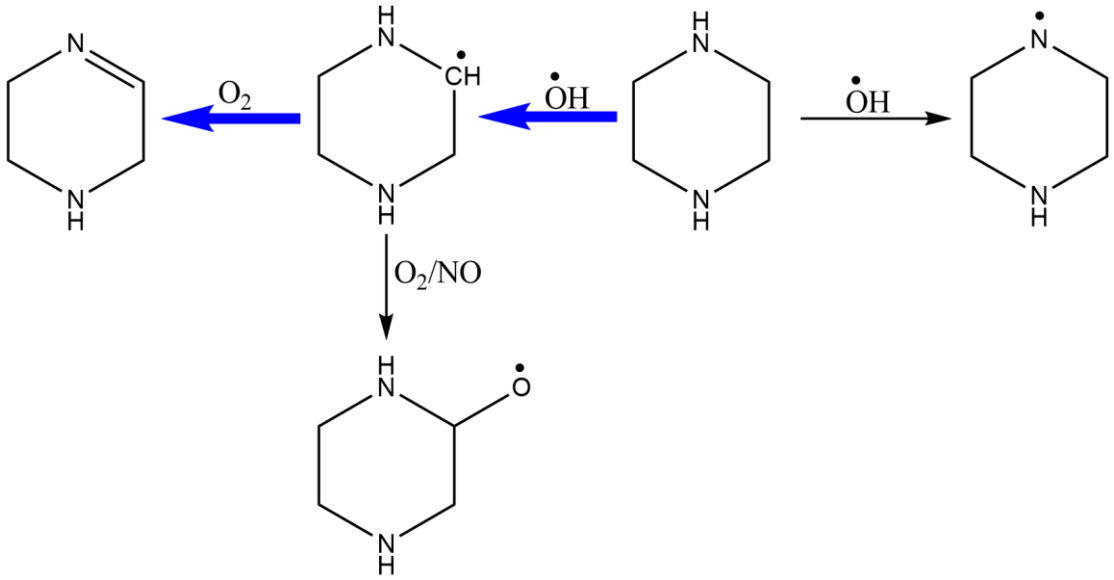

Introduction

Carbon capture technology is being actively pursued as a means of reducing CO_2 emissions from fossil fuel burning.[1-6] Among these technologies, absorption into liquid amine solvents is currently the most mature.[7-10] The amine piperazine (Pz) is one potentially attractive solvent when mixed with other compounds.[7, 11-15] It is inevitable that significant quantities of volatile amines will be released to the atmosphere during their manufacture, transport, and use in any amine-based carbon capture process,[16-19] and we therefore require a thorough understanding of the atmospheric chemistry of piperazine.

Pz is a nitrogen-containing heterocycle with a six-member ring and two secondary amino groups. When released into the atmosphere, Pz is expected to react predominantly with the •OH radical, via abstraction from C—H sites to form an alkyl radical (PzC) or from N—H sites to form an aminyl radical (PzN). The extent of branching to the PzN radical is of particular interest, as aminyl radicals can react with NO and NO_2 to generate toxic nitrosamines and nitramines, respectively.[20-27] On the other hand, α-aminoalkyl radicals such as PzC have been shown to predominantly react with O_2 to produce imines.[28, 29] Experimentally, Pz has been shown to react with •OH mainly via C—H abstraction, although there is limited information on the further reaction products under atmospheric conditions.[11, 30, 31] This motivated us to carry out a theoretical kinetics investigation into the Pz + •OH reaction through multiple reaction stages, to help validate existing experimental results as well as to provide new insight into the ultimate products of atmospheric oxidation.

Methods

The G4 composite model has been used for all ab initio calculations.[32] Frequency calculations confirmed all minima to have zero imaginary frequencies and all transition states to have one imaginary frequency, with intrinsic reaction coordinate calculations used to confirm transition state connectivity. The G4 method was selected as it can accurately predict barrier heights at reasonable computational cost. Gaussian 16 was used for all reported electronic structure calculations.[33]

The MultiWell Program Suite (2017) is used to for statistical reaction rate simulations,[34] on the basis of G4 theory moments of inertia, vibrational frequencies, and energies. RRKM theory is used to calculate microcanonical rate coefficients, $k(E)$. In the sums and densities of state calculations, harmonic oscillators are used to describe the internal degrees of freedom and an active 1D K-rotor and inactive 2D J-rotor are used to treat external degrees of freedom. Barrierless association reactions are described using the restricted Gorin model,[35] where the rate of complex formation is estimated as the dipole-quadrupole capture rate, k_{cap}.[36] The equation used here is $k_{\mathrm{cap}} = C\mu^{-0.5}\left|d\,Q\right|^{1/2}$, where C is a constant, μ is reduced mass, and d and Q are the respective dipole and quadrupole moments. All values are in atomic units and they are included in Supporting Information. The capture rate of Pz and •OH is estimated to be 2.61×10^{-10} cm^3 molecule^{-1} s^{-1}, whereas the capture rate of PzC and O_2 is significantly lower at 3.35×10^{-11} cm^3 molecule^{-1} s^{-1}, largely due to the small quadrupole moment of O_2. Product yields are obtained from time-dependent energy grained master equation simulations. The upper limit of the continuum master equation is set as 150,000 cm^{-1} (well above any barriers or excitation energies) discretized into 2000 grains with size of 10 cm^{-1}. Each simulation featured 10 million trajectories and sufficient collisions to reach steady-state. The Lennard-Jones model is used to

describe the collision of wells with the bath gas, N_2. For the Pz–OH aducts, Lennard-Jones parameters σ and ϵ/k_b are set as 6.2 Å and 584 K. For PzC–O_2 adducts, Lennard-Jones parameters σ and ϵ/k_b are set as 6.04 Å and 524.6 K. The average energy in deactivating collisions, $\Delta E_{down,}$ is set as 100 cm^{-1} in the Pz + •OH reaction and 100 ± 50 cm^{-1} for PzC + O_2.

Results and Discussion

The •OH radical can abstract H from either a N site on Pz, to form a N atom centred aminyl radical (PzN) + H_2O, or a C site on Pz, to form a C atom centred alkyl radical (PzC) + H_2O. A theoretical energy diagram of the Pz + •OH reaction is depicted in **Figure 1**. The optimised geometries of the transition states and wells in the H abstraction are shown in **Figure 2**.

The initial step begins with the approach of •OH radical to Pz, resulting in barrierless and exothermic formation of pre-reaction adduct **1** by 8.1 kcal mol^{-1} or **2** by 4.9 kcal mol^{-1}. From **1** the C—H bond will break via **TS1** which sits 1.4 kcal mol^{-1} above **1** (6.7 kcal mol^{-1} below the reactants). From **2**, the N—H bond will break via transition state **TS2** which is 3.3 kcal mol^{-1} above **2** (1.6 kcal mol^{-1} below Pz + •OH). Additionally, pre-reactant complexes **1** and **2** can interconvert via **TS3**, which sits at close to the energy of **2**. This process predominantly involves rotation of the OH group; the H—O—N—H dihedral changes from almost 0° in **1** to about -112° in **2**, and is -28° in **TS3**. After H abstraction, **TS1** leads to the alky radical (PzC) and H_2O, whereas **TS2** goes to the aminyl radical (PzN) and H_2O in a marginally less exothermic process. According to the potential energy diagram developed here we would expect PzC to be the dominant reaction product, due to both the lower abstraction barrier and the ability for the two pre-reaction complexes to readily interconvert.

In order to quantify the Pz + •OH reaction kinetics, master equation modelling has been carried out from 300 K to 500 K at 1 atm N_2. As is shown in **Figure 3**, the calculated rate coefficient at 300 K matches the experimental result of Onel *et al.*[31] Additionally, the negative activation energy is captured reasonably well.[31] At 300 K, C—H and N—H abstraction rate coefficients are estimated to be $k_{\mathrm{C}abst} = k_{cap} \times y_{\mathrm{C-H}} = 2.38\times10^{-10}$ cm^3 $molecule^{-1}$ s^{-1} and $k_{\mathrm{N}abst} = k_{cap} \times y_{\mathrm{N-H}} = 2.66\times10^{-12}$ cm^3 $molecule^{-1}$ s^{-1} respectively, where $y_{\mathrm{C-H}}$ is the yield of C—H abstraction products and $y_{\mathrm{N-H}}$ is the yield of N—H abstraction products. Predicted branching to C—H abstraction is $k_{\mathrm{C}abst} / (k_{\mathrm{C}abst} + k_{\mathrm{N}abst})$ ≈ 99 %, confirming this as the major reaction channel. As temperature increases from 300 to 500 K, the branching ratio of C—H abstraction remains as the major reaction channel and slightly decreases from 99 % to 94 %. Yields, abstraction rate coefficients, and branching ratios of both channels at 300 to 500 K are listed in Supporting information. Thus, subsequent reactions between PzN and NO or NO_2 which may produce carcinogenic nitrosamines and nitramines are predicted to be minor in the atmospheric oxidation of piperazine initiated by •OH, although due to their potentially acute toxicity they may still need to be included in atmospheric chemical mechanisms.

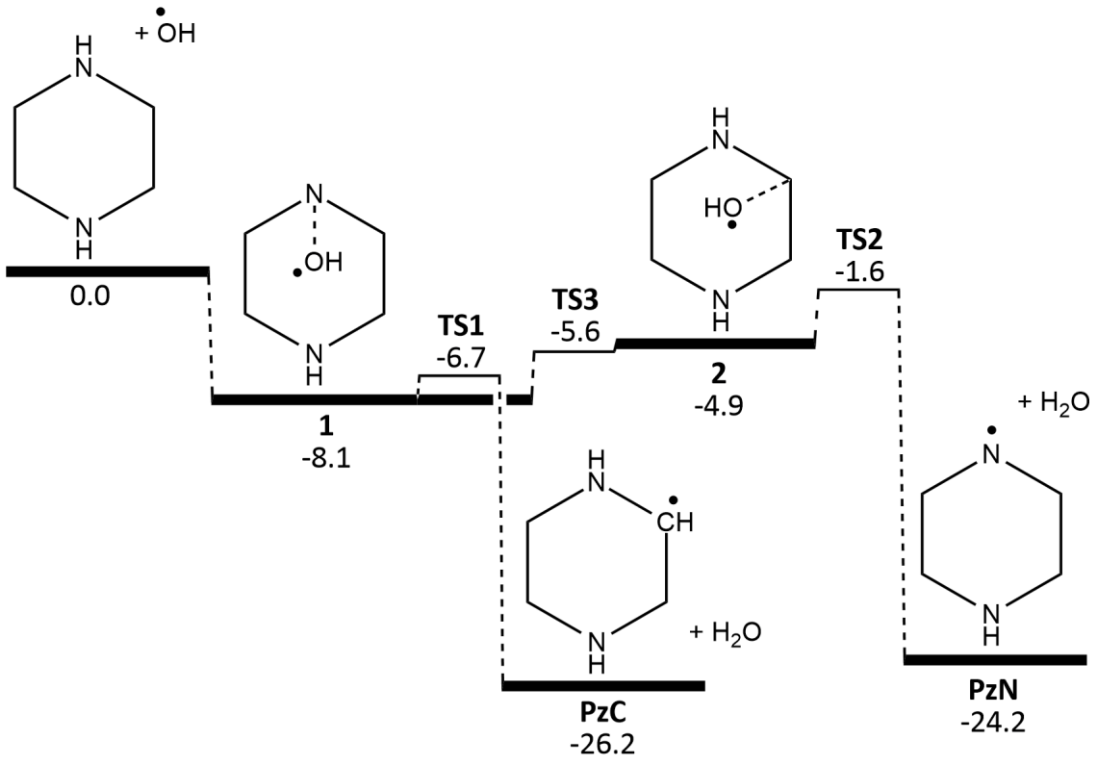

Figure 1. Potential energy diagram for the piperazine + •OH reaction. Relative energies are 0 K enthalpies in the units of kcal mol^{-1}, at the G4 level of theory.

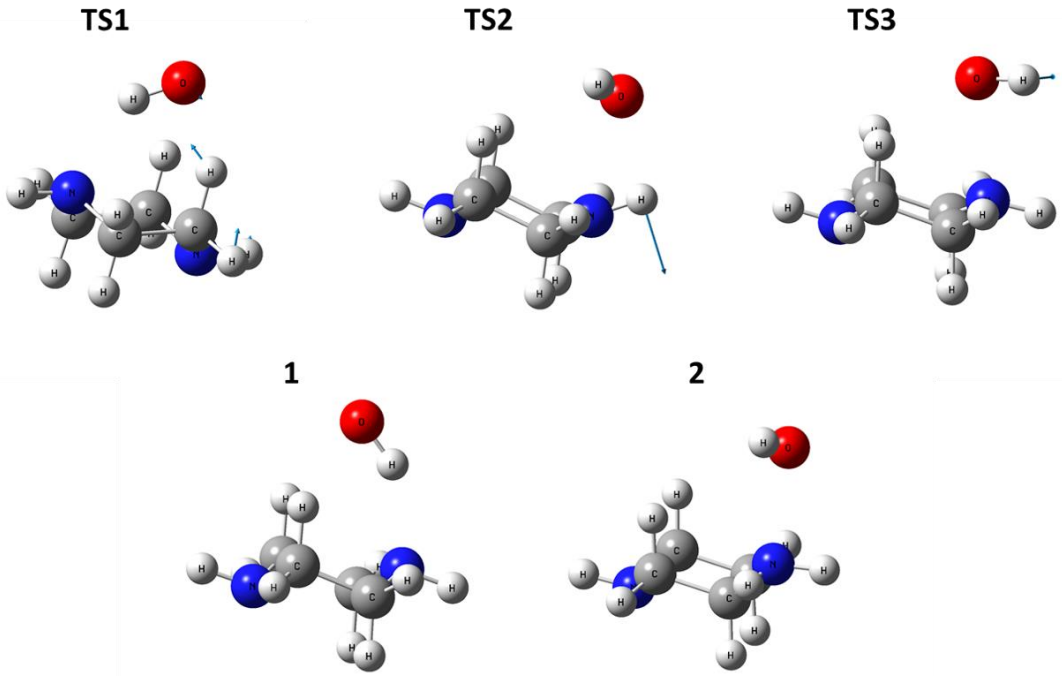

Figure 2. Optimized structures of the wells and transition states of Pz + •OH reaction at G4 level of theory. For the transition states, displacement vectors of the imaginary frequency are included.

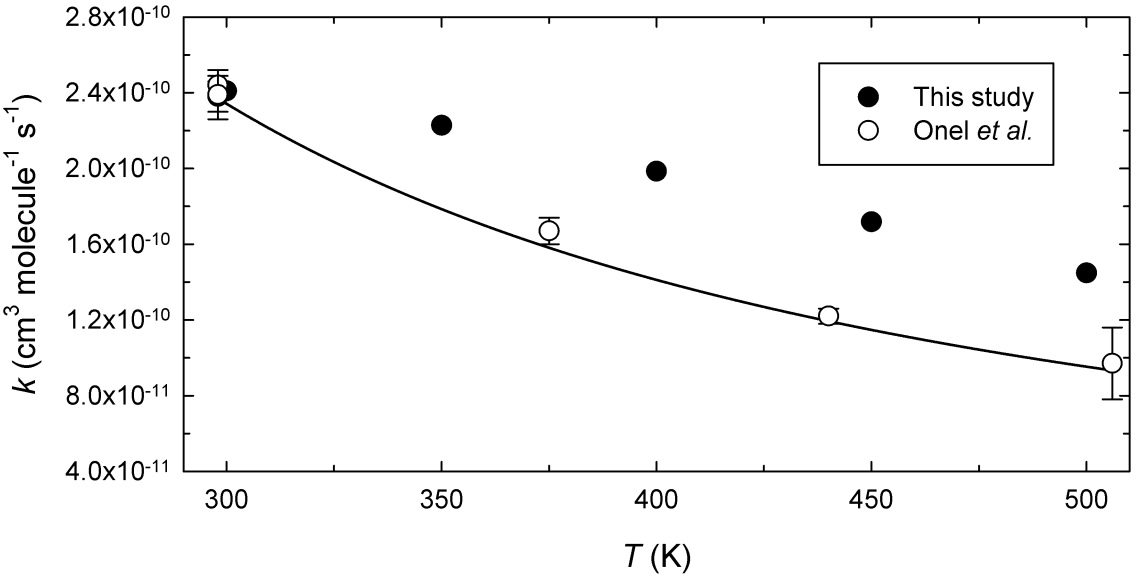

Figure 3. Total rate coefficient (*k*) from calculations and experiments as a function of temperature (*T*) in the Pz + $^{\bullet}$OH reaction.

Once formed, the PzC radical will rapidly react with O_2 in the atmosphere. The energy diagram for the reaction of PzC + O_2 is shown in **Figure 4**. Energies of all the transition states, intermediates and products are below the reactants. The optimised structures of the transition states and wells in the mechanisms are illustrated in **Figure 5**. Firstly, the alkyl radical (PzC) combines with molecular O_2 to form the peroxyl radical ($RO_2^{\bullet}$) intermediate **3**, releasing 35 kcal mol^{-1} in energy. From here, **3** can undergo $HO_2^{\bullet}$ elimination via a five-member ring like transition state, **TS4**, which is 16.4 kcal mol^{-1} below the reactant and 19 kcal mol^{-1} above the peroxyl radical **3**. Following $HO_2^{\bullet}$ elimination there is the formation of a weak post-reactant adduct **4**, which can dissociate to the cyclic imine 1,2,3,6-tetrahydropyrazin and $HO_2^{\bullet}$, whose energies are 14.4 kcal mol^{-1} below the reactants.

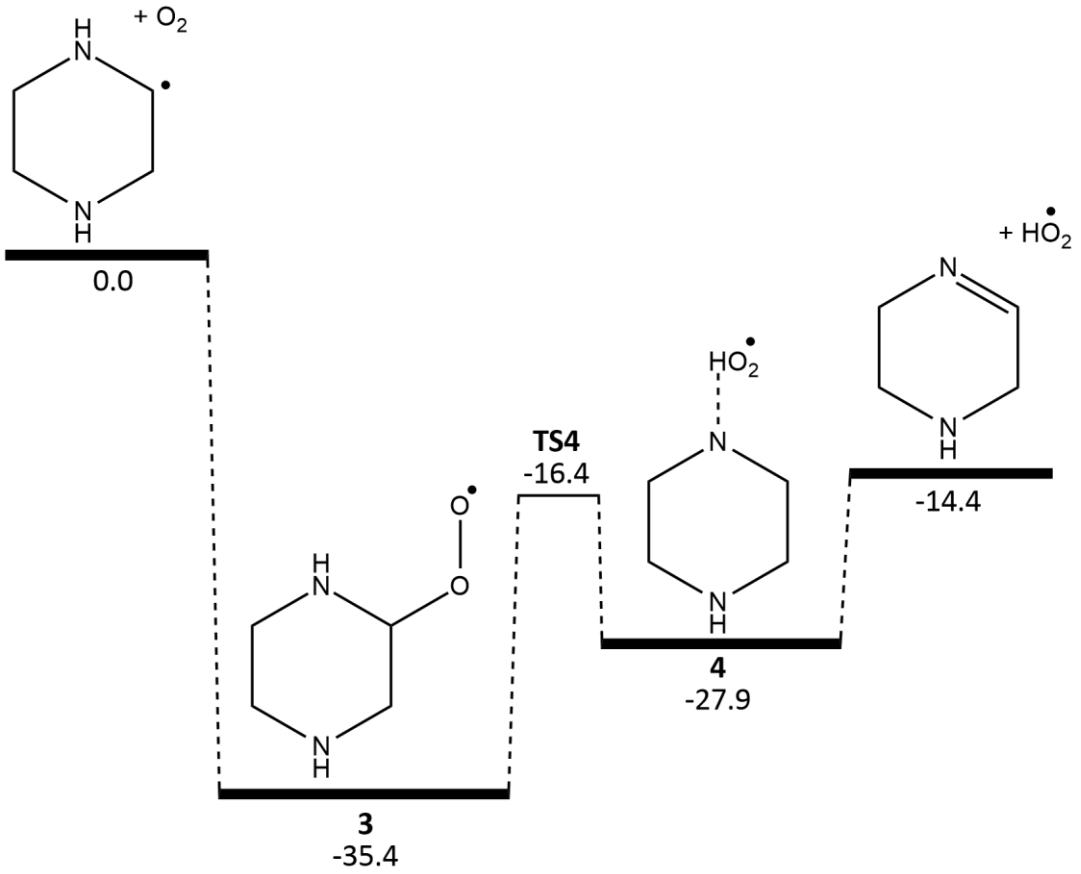

Figure 4. Potential energy diagram for the reaction of PzC + O_2. Relative energies are 0 K enthalpies in the units of kcal mol^{-1}, at the G4 level of theory.

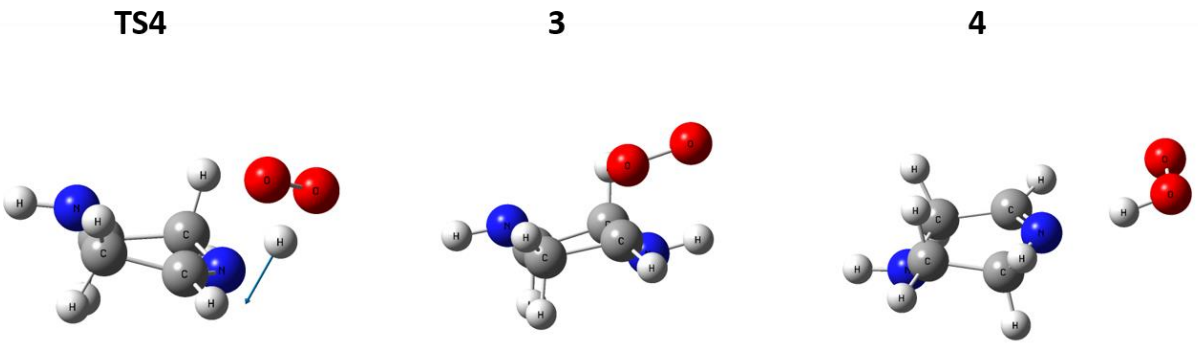

Figure 5. Optimized structures of the wells and transition states of PzC + O_2 reaction at the G4 level of theory. For the transition state, displacement vectors of the imaginary frequency are included.

It is apparent from **Figure 4** that following the association of PzC with O_2, the chemically activated peroxyl radical will have sufficient energy to dissociate to 1,2,3,6-tetrahydropyrazin + $HO_2^{\bullet}$. This process will, however, be in competition with collisional deactivation of the peroxyl radical as well as reverse dissociation to the reactants. To better understand these processes, a master equation model has been developed, and simulations were carried out at 14 Torr (the pressure of the Onel *et al*. study) and 1 atm N_2. At 14 Torr, we predict no peroxyl radical stabilization, supporting the assumption of

Onel *et al*. that PzC was quantitatively oxidised to $HO_2^\bullet$ in their reactor. From the 1 atm simulations we found that the only significant product channels were for peroxyl radical stabilization and dissociation to the imine + $HO_2^\bullet$, although the relative yields were sensitive to the collisional energy transfer model adopted. The time-evolution of peroxyl radical **3** in the PzC + O_2 reaction at 298 K and 1 atm N_2 is plotted in **Figure 6**, for ΔE_{down} = 100 ± 50 cm^{-1}. At 100 cm^{-1} the steady-state peroxyl radical yield is 11.3 %, increasing to 26.9 % at 150 cm^{-1} and dropping to effectively zero at 50 cm^{-1}.

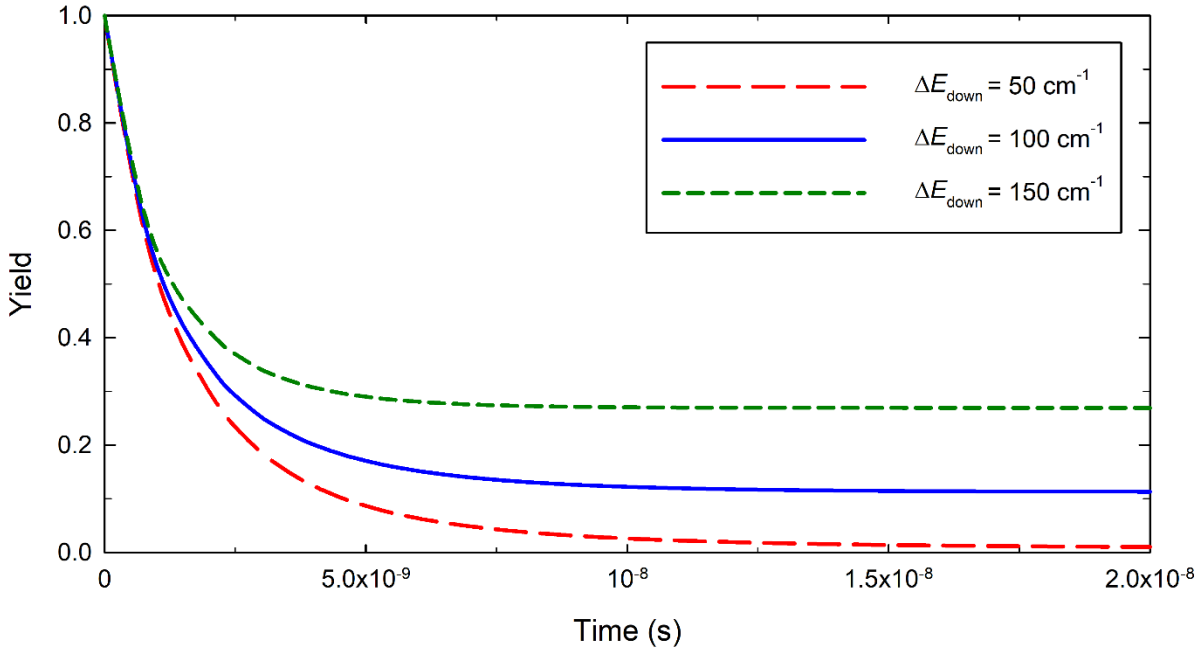

Figure 6. Predicted $RO_2^\bullet$ peroxyl radical yields *vs*. time from master equation simulations at 298 K and 1 atm N_2.

Although not the major product in the atmospheric degradation of Pz, we predict that the peroxyl radical **3** will be formed to some extent, yet its further reaction pathways have to date been unexplored. In polluted environments the dominant fate will be reaction with NO to produce an alkoxyl radical ($RO^\bullet$), **5**, as shown in Eqn (1). The energy release of this process is calculated as 10.0 kcal mol^{-1}, which will provide the $RO^\bullet$ radical with some excess vibrational energy over that of a thermalized population.

$$RO_2^\bullet + NO \rightarrow RO^\bullet + NO_2 \qquad (1)$$

Following the formation of $RO^\bullet$, there is competition between the bimolecular reaction $RO^\bullet$ + O_2 and unimolecular $RO^\bullet$ chemistry. The energy diagram for the $RO^\bullet$ + O_2 reaction is depicted in the Supporting Information; this reaction produces a cyclic amide via a transition state which is 3.1 kcal mol^{-1} above the entrance channel. A diagram illustrating the main isomerisation and decomposition pathways of the alkoxyl radical $RO^\bullet$ are shown in **Figure 7**. The alkoxyl radical can break the C—N bond and form a N-centred radical $HCOCH_2NHCH_2CH_2NH^\bullet$ with a barrier of 14.3 kcal mol^{-1}, from which no further low-energy pathways were identified. Direct C—H beta-scission leading to H loss, forming a cyclic amide, proceeds with a barrier of 8.9 kcal mol^{-1}. The alkoxyl radical can also break the C—C bond via a multistep process (**TS7** – **TS9**) with a barrier lower than both the H loss and C—N bond breaking

reactions. Firstly, the directions of the H—N bonds located at the meta and ortho N atoms sequentially change from equatorial to axial. Then C—C bond cleavage forms a ring-opened structure $HCONHCH_2CH_2NHCH_2^{\bullet}$ via a near-barrierless process. Subsequent H shift reactions of $HCONHCH_2CH_2NHCH_2^{\bullet}$ have also been explored, although all energies are significantly above the entrance channel (see Supporting Information). Accordingly, the main alkoxyl radical product is expected to be the open chain alkyl radical $HCONHCH_2CH_2NHCH_2^{\bullet}$, which can undergo a second O_2 addition mechanism.

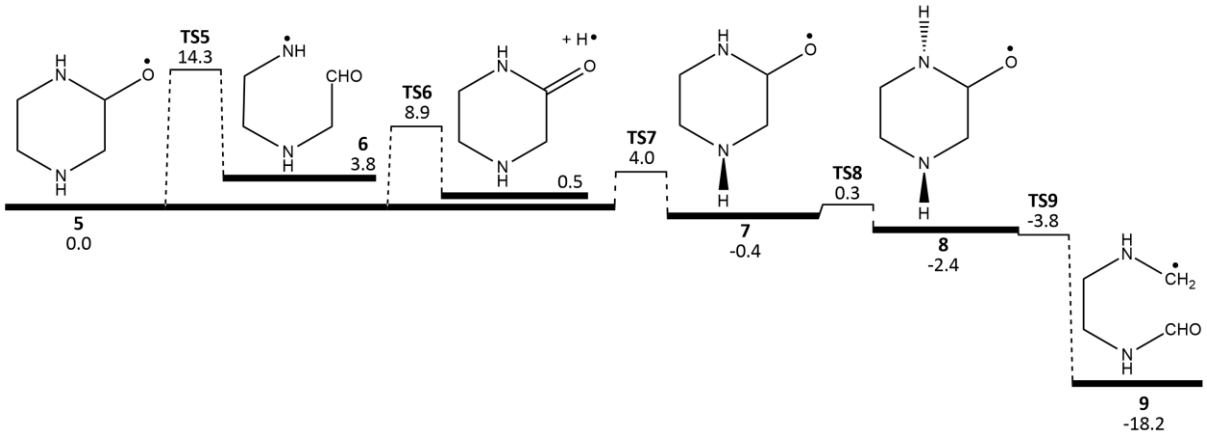

Figure 7. Potential energy diagram for PzC alkoxyl radical isomerisation. Relative energies are 0 K enthalpies in the units of kcal mol^{-1}, at the G4 level of theory.

Similar to the alkyl radical PzC, $HCONHCH_2CH_2NHCH_2^{\bullet}$ reacts with O_2 to form a peroxyl radical (**10**), releasing 33.3 kcal mol^{-1} in energy. Subsequently, **10** can undergo $HO_2^{\bullet}$ elimination via **TS10**, which is 19.4 kcal mol^{-1} above **10** (13.9 kcal mol^{-1} below $HCONHCH_2CH_2NHCH_2^{\bullet} + O_2$). After $HO_2^{\bullet}$ elimination, **TS10** leads to the post-reactant complex **11**, which will dissociate to $CH_2=NCH_2CH_2NHCHO$ and $HO_2^{\bullet}$, whose energies are 12.3 kcal mol^{-1} above well **11** and 13.7 kcal mol^{-1} below the entrance channel. The relevant energy diagram is depicted in **Figure 8**.

Based upon the results presented above, we predict that Pz will react with $^{\bullet}OH$ in the troposphere to almost exclusively produce the carbon-centred radical PzC. Subsequent reaction with O_2 then leads predominantly to the imine 1,2,3,6-tetrahydropyrazin (+ $HO_2^{\bullet}$), but with a stabilised peroxyl radical yield of about 10 %. The corresponding alkoxyl radical can undergo ring opening followed by second O_2 addition to produce an open-chain imine, $CH_2=NCH_2CH_2NHCHO$. These findings are summarized in **Figure 9**.

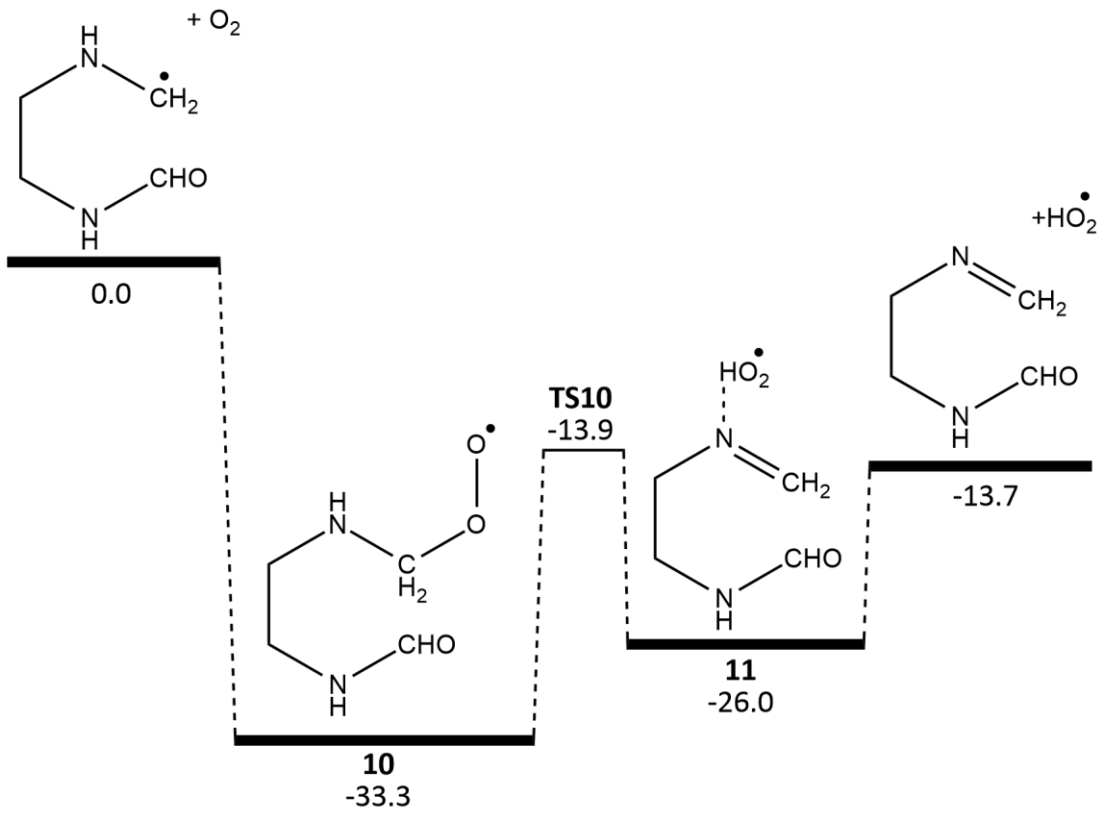

Figure 8. Potential energy diagram for $HCONHCH_2CH_2NHCH_2^{\bullet}$ + O_2 reaction. Relative energies are 0 K enthalpies in the units of kcal mol^{-1}, at the G4 level of theory.

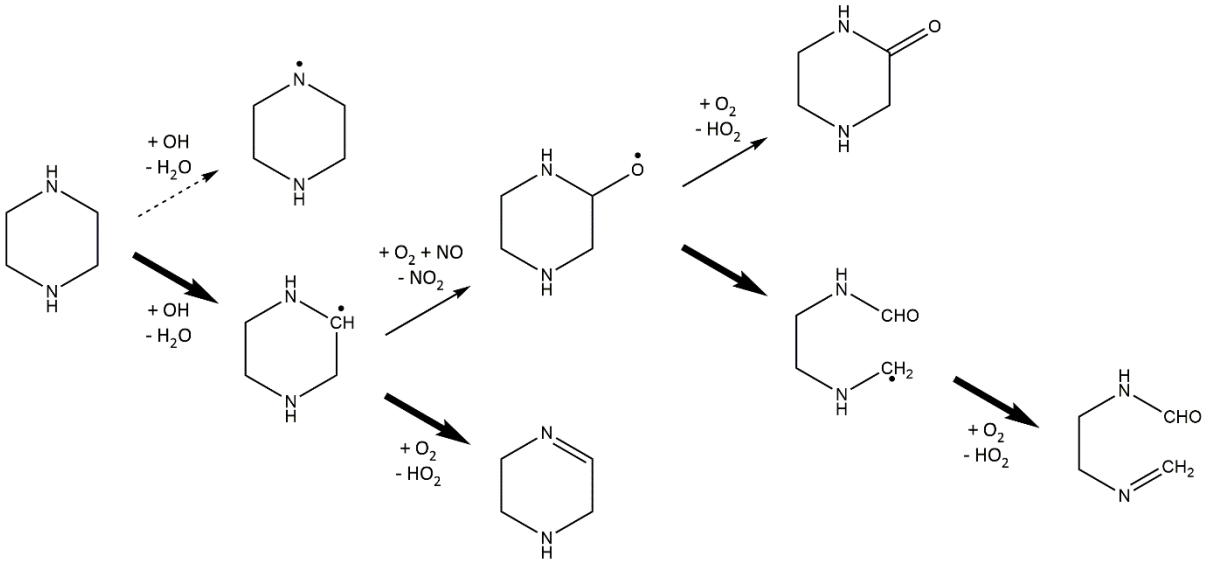

Figure 9. Proposed atmospheric reaction scheme for the $^{\bullet}OH$ radical initiated oxidation of piperazine.

Summary and Conclusions

In this work the $^{\bullet}OH$ initiated atmospheric oxidation of Pz has been studied. H abstraction from C—H sites is found to have a lower barrier than N—H sites, and master equation modelling confirms that H

abstraction happens predominantly on C—H sites. Predicted rate coefficients for the Pz + $^{\bullet}$OH reaction are consistent with experiment. Reaction of the alkyl piperazine radical PzC with O_2 is is also investigated, with the main product predicted to be a cyclic imine produced via a $HO_2^{\bullet}$ elimination process, with minor yield of the stabilized peroxyl radical. The alxokyl radical formed in the reaction of $RO_2^{\bullet}$ + NO can subsequently isomerize and react with a second O_2 to produce CH_2=NCH_2CH_2NHCHO and $HO_2^{\bullet}$.

Supporting Information Available:

Potential energy diagrams for the $RO^{\bullet}$ + O_2 reaction and $HCONHCH_2CH_2NHCH_2^{\bullet}$ isomerisation, parameters used in capture rates calculation and calculated yields, rate coefficients and branching ratios.

Acknowledgements

This work was supported by the Australian Research Council through the Future Fellowships program.

References

1. Haszeldine, R. S., Carbon Capture and Storage: How Green Can Black Be? *Science* **2009,** *325* (5948), 1647-1652.
2. Bui, M.; Adjiman, C. S.; Bardow, A.; Anthony, E. J.; Boston, A.; Brown, S.; Fennell, P. S.; Fuss, S.; Galindo, A.; Hackett, L. A., Carbon capture and storage (CCS): the way forward. *Energy & Environmental Science* **2018,** *11* (5), 1062-1176.
3. Wall, T. F., Combustion processes for carbon capture. *Proceedings of the Combustion Institute* **2007,** *31* (1), 31-47.
4. Cuéllar-Franca, R. M.; Azapagic, A., Carbon capture, storage and utilisation technologies: A critical analysis and comparison of their life cycle environmental impacts. *Journal of CO_2 Utilization* **2015,** *9*, 82-102.
5. Xie, H.-B.; Johnson, J. K.; Perry, R. J.; Genovese, S.; Wood, B. R., A computational study of the heats of reaction of substituted monoethanolamine with CO_2. *The Journal of Physical Chemistry A* **2010,** *115* (3), 342-350.
6. Liu, Y.; Zhang, L.; Watanasiri, S., Representing vapor− liquid equilibrium for an aqueous MEA− CO_2 system using the electrolyte nonrandom-two-liquid model. *Industrial & Engineering Chemistry Research* **1999,** *38* (5), 2080-2090.
7. Thee, H.; Suryaputradinata, Y. A.; Mumford, K. A.; Smith, K. H.; da Silva, G.; Kentish, S. E.; Stevens, G. W., A kinetic and process modeling study of CO_2 capture with MEA-promoted potassium carbonate solutions. *Chemical Engineering Journal* **2012,** *210*, 271-279.
8. Gray, M.; Soong, Y.; Champagne, K.; Baltrus, J.; Stevens Jr, R.; Toochinda, P.; Chuang, S., CO_2 capture by amine-enriched fly ash carbon sorbents. *Separation and Purification Technology* **2004,** *35* (1), 31-36.
9. Lepaumier, H.; Picq, D.; Carrette, P.-L., New amines for CO_2 capture. II. Oxidative degradation mechanisms. *Industrial & Engineering Chemistry Research* **2009,** *48* (20), 9068-9075.
10. Pires, J.; Martins, F.; Alvim-Ferraz, M.; Simões, M., Recent developments on carbon capture and storage: an overview. *Chemical Engineering Research and Design* **2011,** *89* (9), 1446-1460.

11. White, S.; Angove, D.; Azzi, M.; Tibbett, A.; Campbell, I.; Patterson, M., An experimental investigation into the atmospheric degradation of piperazine. *Atmospheric Environment* **2015,** *108*, 133-139.
12. Knudsen, S.; Karl, M.; Randall, S., Amine emissions to air during carbon capture. *Norwegian Institute for Air Research* **2009**.
13. Freeman, S. A.; Dugas, R.; Van Wagener, D. H.; Nguyen, T.; Rochelle, G. T., Carbon dioxide capture with concentrated, aqueous piperazine. *International Journal of Greenhouse Gas Control* **2010,** *4* (2), 119-124.
14. Ma, F.; Xie, H.-b.; Elm, J.; Shen, J.; Chen, J.; Vehkamäki, H., Piperazine Enhancing Sulfuric Acid Based New Particle Formation: Implications for the Atmospheric Fate of Piperazine. *Environmental Science & Technology* **2019**.
15. Rochelle, G.; Chen, E.; Freeman, S.; Van Wagener, D.; Xu, Q.; Voice, A., Aqueous piperazine as the new standard for CO_2 capture technology. *Chemical Engineering Journal* **2011,** *171* (3), 725-733.
16. Nielsen, C. J.; Herrmann, H.; Weller, C., Atmospheric chemistry and environmental impact of the use of amines in carbon capture and storage (CCS). *Chemical Society Reviews* **2012,** *41* (19), 6684-6704.
17. Ge, X.; Wexler, A. S.; Clegg, S. L., Atmospheric amines–Part I. A review. *Atmospheric Environment* **2011,** *45* (3), 524-546.
18. Gouedard, C.; Picq, D.; Launay, F.; Carrette, P.-L., Amine degradation in CO_2 capture. I. A review. *International Journal of Greenhouse Gas Control* **2012,** *10*, 244-270.
19. Zhu, L.; Schade, G. W.; Nielsen, C. J., Real-time monitoring of emissions from monoethanolamine-based industrial scale carbon capture facilities. *Environmental Science & Technology* **2013,** *47* (24), 14306-14314.
20. Låg, M.; Lindeman, B.; Instanes, C.; Brunborg, G.; Schwarze, P., Health effects of amines and derivatives associated with CO_2 capture. *IARC Sci Publ* **1984,** *57*, 3-22.
21. Onel, L.; Thonger, L.; Blitz, M.; Seakins, P.; Bunkan, A.; Solimannejad, M.; Nielsen, C., Gas-phase reactions of OH with methyl amines in the presence or absence of molecular oxygen. An experimental and theoretical study. *The Journal of Physical Chemistry A* **2013,** *117* (41), 10736-10745.
22. Dai, N.; Shah, A. D.; Hu, L.; Plewa, M. J.; McKague, B.; Mitch, W. A., Measurement of nitrosamine and nitramine formation from NOx reactions with amines during amine-based carbon dioxide capture for postcombustion carbon sequestration. *Environmental Science & Technology* **2012,** *46* (17), 9793-9801.
23. Ma, F.; Ding, Z.; Elm, J.; Xie, H.-B.; Yu, Q.; Liu, C.; Li, C.; Fu, Z.; Zhang, L.; Chen, J., Atmospheric Oxidation of Piperazine Initiated by ·Cl: Unexpected High Nitrosamine Yield. *Environmental Science & Technology* **2018,** *52* (17), 9801-9809.
24. Onel, L.; Blitz, M.; Dryden, M.; Thonger, L.; Seakins, P., Branching ratios in reactions of OH radicals with methylamine, dimethylamine, and ethylamine. *Environmental Science & Technology* **2014,** *48* (16), 9935-9942.
25. Gao, H.; Wang, M.; Jin, T.; Shi, J.; Yao, X.; Jin, N., Direct dynamics study on hydrogen abstraction reaction of morpholine with hydroxyl radical. *Theoretical Chemistry Accounts* **2015,** *134* (8), 96.
26. Goldman, M. J.; Fine, N. A.; Rochelle, G. T., Kinetics of N-nitrosopiperazine formation from nitrite and piperazine in CO_2 capture. *Environmental Science & Technology* **2013,** *47* (7), 3528-3534.
27. Nicovich, J. M.; Mazumder, S.; Laine, P. L.; Wine, P. H.; Tang, Y.; Bunkan, A. J.; Nielsen, C. J., An experimental and theoretical study of the gas phase kinetics of atomic chlorine reactions with CH_3NH_2, $(CH_3)_2NH$, and $(CH_3)_3N$. *Physical Chemistry Chemical Physics* **2015,** *17* (2), 911-917.

28. da Silva, G.; Kirk, B. B.; Lloyd, C.; Trevitt, A. J.; Blanksby, S. J., Concerted HO_2 elimination from α-aminoalkylperoxyl free radicals: Experimental and theoretical evidence from the gas-phase NH_2•$CHCO_2^-$ + O_2 reaction. *The Journal of Physical Chemistry Letters* **2012,** *3* (7), 805-811.
29. Tang, Y.; Nielsen, C. J., A systematic theoretical study of imines formation from the atmospheric reactions of RnNH2− n with O2 and NO2 (R= CH3 and CH3CH2; n= 1 and 2). *Atmospheric environment* **2012,** *55*, 185-189.
30. Nielsen, C. J.; Bossi, R.; Bunkan, A. J. C.; Dithmer, L.; Glasius, M.; Hallquist, M.; Hansen, A. M. K.; Lutz, A.; Salo, K.; Maguta, M. M., Atmospheric Degradation of Amines (ADA): summary report from atmospheric chemistry studies of amines, nitrosamines, nitramines and amides. **2012**.
31. Onel, L.; Dryden, M.; Blitz, M. A.; Seakins, P. W., Atmospheric oxidation of piperazine by OH has a low potential to form carcinogenic compounds. *Environmental Science & Technology Letters* **2014,** *1* (9), 367-371.
32. Curtiss, L. A.; Redfern, P. C.; Raghavachari, K., Gaussian-4 theory. *The Journal of Chemical Physics* **2007,** *126* (8), 084108.
33. Frisch, M.; Trucks, G.; Schlegel, H.; Scuseria, G.; Robb, M.; Cheeseman, J.; Scalmani, G.; Barone, V.; Petersson, G.; Nakatsuji, H., Gaussian 16. *Revision A* **2016,** *3*.
34. Barker, J.; Nguyen, T.; Stanton, J.; Aieta, C.; Ceotto, M.; Gabas, F.; Kumar, T.; Li, C.; Lohr, L.; Maranzana, A., MultiWell-2017 Software Suite. *Ann Arbor, Michigan* **2017**.
35. Smith, G.; Golden, D., Application of RRKM theory to the reactions OH + NO_2 + N_2 → $HONO_2$ + N_2 (1) and ClO + NO_2 + N_2 → $ClONO_2$ + N_2 (2); a modified gorin model transition state. *International Journal of Chemical Kinetics* **1978,** *10* (5), 489-501.
36. Georgievskii, Y.; Klippenstein, S. J., Long-range transition state theory. *The Journal of Chemical Physics* **2005,** *122* (19), 194103.